Bioorganic & Medicinal Chemistry 21 (2013) 6077–6083

Contents lists available at SciVerse ScienceDirect

Bioorganic & Medicinal Chemistry

journal homepage: www.elsevier.com/locate/bmc

Design and synthesis of (4*E*)-4-(4-substitutedbenzylideneamino)-3-substituted-2,3-dihydro-2-thioxothiazole-5-carbonitrile as novel A_{2A} receptor antagonists

Chandra Bhushan Mishra, Dimpy Sharma, Amresh Prakash, Namrata Kumari, Nitin Kumar, Pratibha Mehta Luthra *

Neuropharmaceutical Laboratory, Dr. B.R. Ambedkar Center for Biomedical Research, University of Delhi, North Campus, Mall Road, Delhi 110 007, India

ARTICLE INFO

Article history:
Available online 13 July 2013

Keywords:
A_{2A}R antagonist
Radioligand-binding assay
cAMP assay
Haloperidol
2-Thioxothiazole

ABSTRACT

Novel 2-thioxothiazole derivatives (**6**–**19**) as potential adenosine A_{2A} receptor (A_{2A}R) antagonists were synthesized. The strong interaction of the compounds (**6**–**19**) with A_{2A}R in docking study was confirmed by high binding affinity with human A_{2A}R expressed in HEK293T cells using radioligand-binding assay. The compound **19** demonstrated very high selectivity for A_{2A}R as compared to standard A_{2A}R antagonist SCH58261. Decrease in A_{2A}R-coupled release of endogenous cAMP in treated HEK293T cells demonstrated in vitro A_{2A}R antagonist potential of the compound **19**. Attenuation in haloperidol-induced impairment (catalepsy) in Swiss albino male mice pre-treated with compound **19** is evocative to explore its prospective in therapy of PD.

1. Introduction

Adenosine, an endogenous ligand interacts with adenosine receptor to perform variety of physiological and pathological conditions.[1] Four mammalian adenosine receptor subtypes (A_1R, A_{2A}R, A_{2B}R, and A_3R), belonging to GPCR superfamily, have been characterized.[2,3] Adenosine A_{2A} receptors (A_{2A}R) have emerged as promising nondopaminergic target to control the motor impairment effect of PD.[4] A_{2A}R antagonists reversed Parkinsonian motor deficits in preclinical models without inducing or exacerbating dyskinesias in nonhuman primate models[5] due to blockade of A_{2A}R co-expressed with D_2R in striatopallidal neurons, which inhibited the release of GABA in the globus pallidus, ultimately leading to enhanced motor function through indirect motor pathway of the basal ganglia.[6]

Several potent and selective A_{2A}R antagonists of structural variability have been synthesized[7,8] (Fig. 1). However, xanthine compounds such as KW6002 were unsuccessful in clinical trials,[9] and nonxanthine compounds such as SCH58261 suffered from lower selectivity, solubility and pharmacokinetic profile.[10] To overcome the existing drawbacks, the development of novel A_{2A} receptor antagonists is essentially desired. Our research group has been intensely engaged to the development of potent and selective A_{2A}R antagonist. In the present paper, we have designed and carried the synthesis of the substituted thioxo-thiazoles as novel A_{2A}R antagonists.

Thiazole ring imparts vital role in metabolic pathways and emerged as important synthon to generate variety of NCEs (new chemical entities) due to highly reactive acidic C-2. Diverse modifications of thiazole ring at various positions led to variety of novel compounds, with wide spectrum of biological activities such as antioxidant,[11] anti inflammatory,[11] and neuro protective.[12] PI_3 kinase modulatory thiazolo[4,5-*g*]dihydroindazoles, HIV-integrase inhibitory thiazolo[5,4-*b*]pyrimidine-5(4*H*)-ones and GSK-3 inhibitory thiazole[5,4-*f*]quinazolin-9-ones[13] revealed therapeutic potential in various diseases. Riluzole, a novel neuroprotective drug, approved for the treatment of amyotrophic lateral scleroses possesses aminothiazole moiety.[14] Hofman Le Roche has developed benzothiazole derivative ASN115 (tozadent) as potent A_{2A}R antagonist, which is in phase II clinical trials now.[15] Previously, we have reported bicyclic thiazolo-pyrimidines and tricyclic thiazolo-triazolo-pyrimides as potent A_{2A}R antagonists.[16–19] In the course of development, it was found that thioxothiazole moiety of bicyclic thiazolo-pyrimidine and tricyclic triazolo-thiazolo-pyrimidine was actively involved in interaction with receptor. Ring sulfur of 2-thioxo thaizole moiety formed key interaction with amino acid N253 at active site of A_{2A}R. Therefore, novel monocyclic compounds possessing 2-thioxo thiazole moiety were developed as novel A_{2A}R antagonists. The criterion of terminal hydrophoric cores with polar central features from pharmacophore modeling studies was incorporated in the design of novel monocyclic thiazole derivatives. (4*E*)-4-(4-Substitutedbenzylideneamino)-3-

* Corresponding author. Tel.: +91 11 27662778; fax: +91 11 27666248.
E-mail address: pmlsci@yahoo.com (P.M. Luthra).

0968-0896/$ - see front matter © 2013 Elsevier Ltd. All rights reserved.
http://dx.doi.org/10.1016/j.bmc.2013.07.005

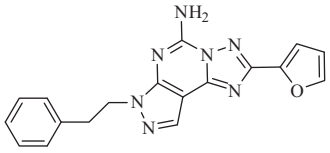

SCH58261

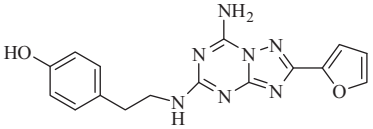

ZM241385

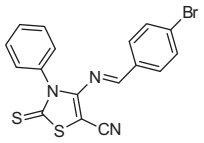

19

Figure 1. Chemical structure of standard $A_{2A}R$ antagonist and synthesized compound **19**.

substituted-2,3-dihydro-2-thioxothiazole-5-carbonitrile (**6**–**19**) were synthesized. N3-hydrophobic and electron rich polar feature of thiazole ring were used as starting material to incorporate N-4 hydrophobic terminal for optimal interaction at active site of $A_{2A}R$.

In vitro radioligand-binding assay was carried using membranes isolated from transfected HEK293T cells with human $A_{2A}R$ to evaluate the binding affinity and selectivity of the compounds (**6**–**19**), the results were comparable to docking analysis. Decrease in endogenous cAMP concentrations in treated HEK293T cells and restoration of locomotor activity in haloperidol-induced mice model was determined for the compound **19**, which possessed maximum binding affinity and selectivity in vitro study.

2. Results and discussion

2.1. Synthesis

The synthesis of compounds **1**–**5** was carried according to previously reported method.[16] The compounds (4*E*)-4-(4-substitutedbenzylideneamino)-3-substituted-2,3-dihydro-2-thioxothiazole-5-carbonitrile (**6**–**19**) were prepared using equimolar mixture of 4-amino-N3-substituted-2, 3-dihydro-2-thioxothiazole-5-carbonitrile (**1**–**5**) and p-substituted benzaldehyde with small amount of $AlCl_3$ in chloroform. Crude product was purified by column chromatography using petroleum ether and ethyl acetate (2:1) as solvent. The compounds (**6**–**19**) were characterized by IR, NMR and mass spectroscopy (Scheme 1).

2.2. Docking analysis

The interaction of thiazole derivatives **6**–**19** and known $A_{2A}R$ antagonist ZM241385 was studied with recently solved X-ray crystal structure of human $A_{2A}R$ (PDB ID: 3EML). The $A_{2A}R$ (3EML) binding cavity is comprised of TM2 (A63, I66), TM3 (A81, V84, L85), ECL2 (F168, E169), ECL3 (H 264, W268), TM5 (M174, M177) and TM6 (W246, L249, N253). Docking simulation results showed that the synthesized (4*E*)-4-(4-substitutedbenzylideneamino)-3-substituted-2,3-dihydro-2-thioxothiazole-5-carbonitrile derivatives (**6**–**19**) and ZM241385 shared a similar binding motif inside the transmembrane (TM) region and extracellular loops of the human $A_{2A}R$ similar to the co-crystallized ZM241385. The binding interaction of (4*E*)-4-(4-bromobenzylideneamino)-N3-phenyl-2,3-dihydro-2-thioxothiazole-5-carbonitrile (**19** as one of the representatives) showed that the sulfur atom of thiazole ring was oriented towards the N253, M177 and V178 (Fig. 2). The involvement of exocyclic sulfur to form H-bond interaction with amide moiety of N253 was analogous to N-1 nitrogen at 7-position of ZM241385. Furthermore, the key receptor residues F168, E169 from ECL2 formed aromatic stacking and hydrophobic polar interaction with N3 position substituent of 2-thioxo-thiazole derivatives **6**–**19**. Overall, thiazole scaffold possessed orientation and contacts almost similar to ZM241385. The bromobenzylidene (hydrophobic group) of **19** was found to be tilted and deep fixed in lower hydrophobic domain of $A_{2A}R$. Nitrogen of carbonitrile and bromobenzylideneamine was involved in polar interaction

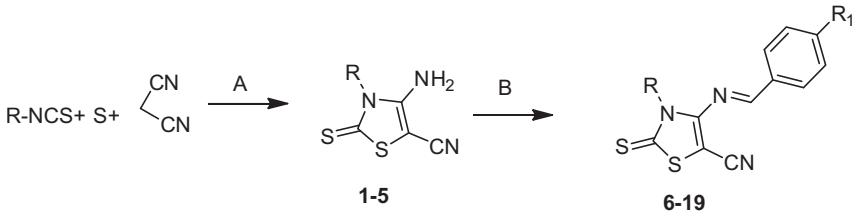

1-5 **6-19**

6.R= Ethyl, R_1= F 11.R= Ethyl , R_1= Cl 16. R=Propyl, R1= Br

7. R= Propyl, R_1=F 12. R=Propyl, R_1= Cl 17. R=Butyl, R_1= Br

8. R=Butyl, R_1= F 13.R=Butyl, R_1= Cl 18. Phenyl ethyl, R_1= Br

9.R= Phenyl ethyl, R_1= F 14.R= Phenyl , R1= Cl 19. R=Phenyl, R_1= Br

10. R= Phenyl, R_1= F 15. R=Ethyl, R1= Br

Scheme 1. Reagents and conditions: (A) TEA, DMF, RT. (B) Substituted benzaldehyde, chloroform, $AlCl_3$, RT.

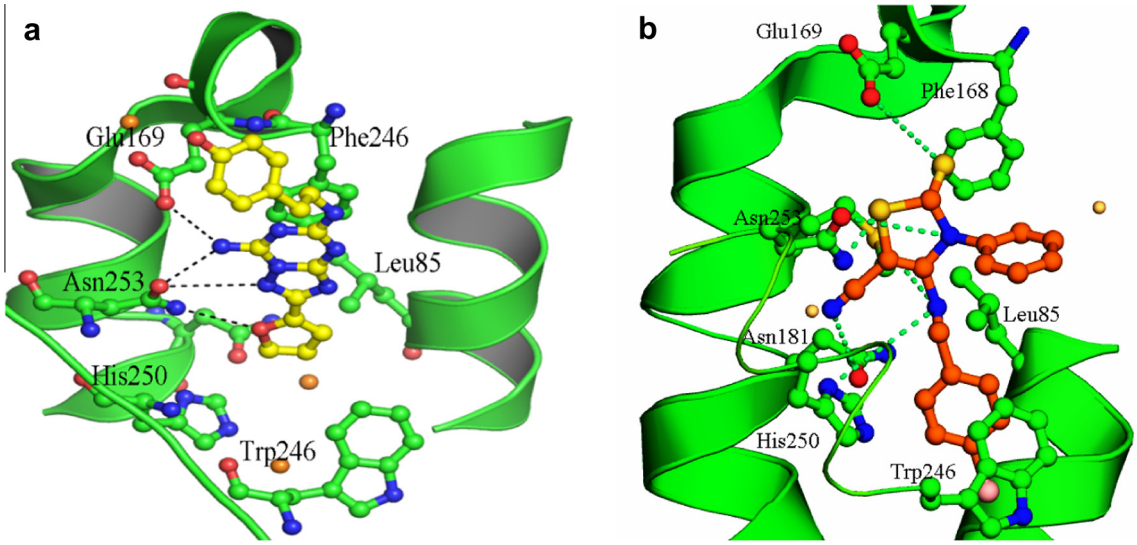

Figure 2. Docking analysis of ZM241385 and compound **19** with crystal structure of $A_{2A}R$ (cartoon view at PyMOL). (a) Standard antagonist ZM241385. (b) The compound **19** (polar interactions are represented with black and green dotted lines). Yellow dotes represented the water molecules present in $A_{2A}R$ active site.

with N181 and H250, respectively. The N3-phenyl ring exhibited π–π hydrophobic interaction with F168.

2.3. Structure–activity relationship

Radioligand binding study of (4*E*)-4-(4-fluorobenzylideneamino)-N3-substituted-2,3-dihydro-2-thioxothiazole-5-carbonitrile series (**6**–**10**) revealed that N3-propyl, N3-butyl and N3-ethylphenyl derivatives possessed selectivity for $A_{2A}R$, however, N3-ethyl derivative (**6**) was highly selective for A_1 receptor (A_1/A_{2A} = 0.000053) and N3-phenyl derivative (**10**) showed strong affinity with both $A_{2A}R$ (K_i = 0.0047 nm) and A_1R (K_i = 0.00063 nm) with some selectivity for $A_{2A}R$ receptor (A_1/A_{2A} = 0.13). Overall order of selectivity profile of the compounds **6**–**10** for $A_{2A}R$ was C_3H_7 (A_1/A_{2A} = 3393) > C_4H_9 (A_1/A_{2A} = 618) > CH_2CH_2Ph (A_1/A_{2A} = 336) > Ph (A_1/A_{2A} = 0.13) > C2H5 (A_1/A_{2A} = 0.000053). In (4*E*)-4-(4-chlorobenzylideneamino)-N3-substituted-2,3-dihydro-2-thioxothiazole-5-carbonitrile series (**11**–**14**), the N3-butyl ($A_1/A_{2A}R$ = 2565) and N3-phenyl ($A_1/A_{2A}R$ = 2947) derivatives were highly selective for $A_{2A}R$. Moreover, the selectivity order of N3-ethyl (**11**) and N3-propyl (**12**) derivatives was found to be reversed. N-3-propyl derivative (**12**) exhibited more binding affinity for A_1R (K_i = 2 nM) as compared to $A_{2A}R$ (K_i = 55 nM; A_1/A_{2A} R = 0.042), however, ethyl derivative (**11**) showed more affinity (K_i = 1.44 nm; A_1/A_{2A} = 13.76) for $A_{2A}R$ (Table 1). N-butyl (**13**, K_i = 9.6 nM, A_1/A_{2A} = 2565) and N-phenyl (**14**, K_i = 0.14 nM, A_1/A_{2A} = 2947) showed high selectivity and affinity for $A_{2A}R$ over A_1R. (4*E*)-4-(4-Bromobenzylideneamino)-N3-substituted-2,3-dihydro-2-thioxothiazole-5-carbonitrile series (**15**–**19**), the order of binding affinity is Ph (**19**, K_i = 0.0042 nM) > C_2H_5 (**15**, K_i = 0.01 nM) > CH_2CH_2Ph (**18**, K_i = 0.067 nM) > C_3H_7 (**16**, K_i = 1.8 nM) > C_4H_9 (**17**, K_i = 7.61), however selectivity profile for $A_{2A}R$ is **19** (A_1/A_{2A} = 44285) > **16** (A_1/A_{2A} = 337) > **18** (A_1/A_{2A} = 4) > **15** (A_1/A_{2A} = 0.074) > **17** (A_1/A_{2A} = 0.13).

The results showed that amongst the (4*E*)-4-(4-fluorobenzylideneamino)-N3-substituted-2,3-dihydro-2-thioxothiazole-5-carbonitrile (**6**–**10**), (4*E*)-4-(4-chlorobenzylideneamino)-3-substituted-2,3-dihydro-2-thioxothiazole-5-carbonitrile (**11**–**14**), and (4*E*)-4-(4-bromobenzylideneamino)-3-substituted-2,3-dihydro-2-thioxothiazole-5-carbonitrile (**15**–**19**), the fluoro substitution contributes only -I effect, chloro substitution imparts -I and mesomeric effect and bromo substitution exhibit mostly mesomeric effect. The optimum carbon length at N terminal is propyl if -I effect prevails (compound **7**), butyl or phenyl if -I and mesomeric effects operate (compounds **13** and **14**), however, only mesomeric effect in N3-phenyl (**19**) makes most selective compound in the series. The comparison of N3-phenyl substituent in fluoro (**10**), chloro (**14**) and bromo (**19**) series showed that the change from -I effect of the fluoro (compound **10**, K_i = 0.0047 nm, A_1/A_{2A} = 0.13) followed by -I effect and mesomeric effect of chloro (**14**, K_i = 0.14 nM, A_1/A_{2A} = 2947) to mesomeric effect of bromo (**19**, K_i = 0.0042 nM, A_1/A_{2A} = 44285) essentially induced the modulation in the conformation of adenosine receptors. Moreover, prevalent mesomeric effect did not affect the affinity with $A_{2A}R$, but decreased the affinity with A_1 receptor (10^6 times) from compounds **6**–**19** (Table 1, such as **10**, K_i = 0.00063 nm; **14**, K_i = 412 nm; **19**, K_i = 186). In the total 14 compounds, four compounds (**7**, **13**, **14**, and **19**) possessed both

Table 1
In-vitro radioligand binding assay for the compounds (**6**–**19**)

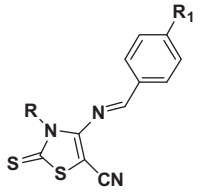

No	R group	R_1 group	K_i A_{2A} (nM)	K_i A_1 (nM)	A_1/A_{2A}
6	Ethyl	Fluro	10.98	0.00059	0.000053
7	Propyl	Fluro	0.03	101.8	3393.3
8	Butyl	Fluro	0.027	16.7	618.51
9	Phenyl ethyl	Fluro	2.64	889.2	336.81
10	Phenyl	Fluro	0.0047	0.00063	0.13
11	Ethyl	Chloro	1.44	19.82	13.76
12	Propyl	Chloro	54.8	2.32	0.042
13	Butyl	Chloro	9.60	24630.0	2565.62
14	Phenyl	Chloro	0.14	412.7	2947.85
15	Ethyl	Bromo	0.01	0.00074	0.074
16	Propyl	Bromo	1.8	606.7	337.05
17	Butyl	Bromo	7.61	0.10	0.013
18	Phenyl ethyl	Bromo	0.067	0.25	3.73
19	Phenyl	Bromo	0.0042	186.0	44285.71

high binding affinity and selectivity, though **19** was most selective compound for $A_{2A}R$ in this series. It has been reported that the communication between ligand and receptor is based on electrostatic interaction, although a stacking interaction operating in the molecular recognition event has been hypothesized. The fluoro-substituent has been reported to alter the electronic distribution in the substrate and changes the conformation without affecting the main values. The size of the substituent modulates the molecular volume determined on the C(aromatic)-substituent bond length of the substituent, that is, chloro (1.747 Å) versus bromo (1.899 Å), resulting in increased steric interaction and therefore an increased energy barrier.[20] In agreement of reported studies, our work has demonstrated that the changes in the electron distribution significantly influenced the electrostatic interaction to induce conformational changes in the adenosine receptors.

Most active and selective compound **19** was selected for cAMP functional assay. In functional assay, binding of ligands to $A_{2A}Rs$ promotes GPCR mediated conformational change via Gαs or Gαi/o subfamily to modulate the activity of adenylate cyclase and alter the concentration of cAMP. An antagonist generally interacts with $A_{2A}R$ via Gαi/o subfamily to inhibit the activity of adenylate cyclase leading to decrease in the cAMP concentration. In this study, NECA stimulated HEK293T cells treated with compound **19** displayed reduction in cAMP concentration (0.56 pmol/ml) as compared to NECA (cAMP concentrations 0.65 pmol/ml). The results were comparable to NECA stimulated HEK293T cells treated with SCH58261 (0.55 pmol/ml).

2.4. Haloperidol induced catalepsy

Four different doses of compound **19** (5, 10 15 and 20 mg/kg) were considered to study haloperidol (2.5 mg/kg) induced catalepsy in Swiss albino male mice. The haloperidol (2.5 mg/kg) treated mice showed high catalepsy score of 2.875 ± 0.125 after 120 min. SCH 58261 pre-treated mice exhibited significant recovery in haloperidol-induced catalepsy (0.625 ± 0.125) after 120 min. Compound **19** pre-treated mice at the dose of 5, 10, 15, 20 mg/kg exhibited catalepsy score of 0.75 ± 0.144, respectively, after 120 min (Fig. 3). The saline treated and 1% acacia in saline treated (control) mice as well as mice treated with compound **19** alone exhibited zero catalepsy score up to 120 min. The results demonstrated that the attenuation of catalepsy score in compound **19** pre-treated haloperidol-induced mice at the dose of 10 mg/kg (0.75 ± 0.144) was significantly higher as compared to SCH58261 (0.65 ± 0.125).

2.5. Conclusion

Novel 2-thioxo thiazole derivatives (**6**–**19**) demonstrated their potential as potent and selective $A_{2A}R$ antagonists. The compounds (**6**–**19**) shared active site binding pocket identical to ZM241385 in docking study. In vitro radioligand binding results showed that the electrostatic interactions largely influenced the binding affinity. However, (4*E*)-4-(4-bromobenzylideneamino)-3-phenyl-2,3-dihydro-2-thioxothiazole-5-carbonitrile **19** displayed both higher binding affinity and selectivity for $A_{2A}R$ in comparison to standard $A_{2A}R$ antagonist SCH58261, antagonized the $A_{2A}R$-coupled release of endogenous cAMP from HEK293T cells and restored haloperidol-induced hypo-locomotors behavior (catalepsy) in vivo to produce motor stimulant effects, further accentuate the potential of 2-thioxo-thiazoles (**6**–**19**) in the treatment of PD.

3. Experimental methodology

The compounds were characterized by TLC, IR, ^{1}H NMR, ^{13}C NMR, and mass spectroscopy. TLC was carried out on commercially available TLC plates (Silica Gel 60 F254, Merck, Germany). IR spectra were performed on Spectrum BX FTIR, PerkinElmer. NMR spectra were recorded on AC Bruker 400 MHz spectrometer in $CDCl_3$ or DMSO. Mass spectra were recorded on a QSTAR XL LC–MS–MS, Applied Biosystem. Melting points were determined using model KSPII, KRUSS, Germany. Elemental analysis was performed on Ementar analysen systeme. Column chromatography purifications were performed using silica gel (100–200 mesh, Merck).

3.1. General procedure for synthesis of 4-amino-N3-substituted-2-thioxo-1,3-thiazole-5-carbonitrile (1–5)

The compounds **1**–**5** were synthesized according to reported method of Luthra et al.[16] Briefly, an equimolar mixture of N-substituted isothiocyanates, malononitrile and sulfur powder in dimethylformamide was stirred in ice bath, added triethylamine dropwise after 15 min, and the stirring was continued for 4 h. The reaction mixture was poured in water, the obtained precipitate was crystallized from absolute ethanol to give 4-amino-3-substituted-2-thioxo-2,3-dihydro-thiazole-5-carbonitrile derivatives (**1**–**5**).

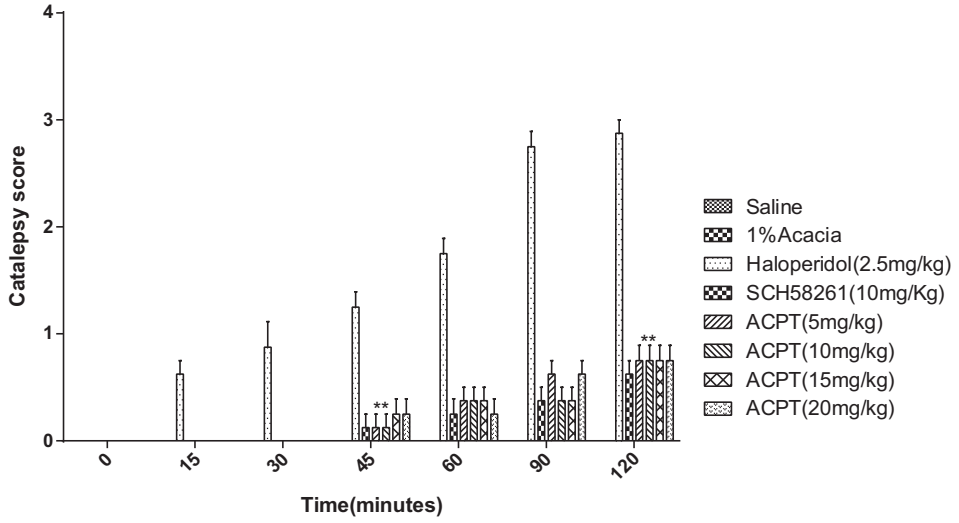

Figure 3. Effect of (4*E*)-4-(4-bromobenzylideneamino)-3-phenyl-2,3-dihydro-2-thioxothiazole-5-carbonitrile at 5, 10, 15 and 20 mg/kg on haloperidol (2.5 mg/kg) induced catalepsy in mice. Results are given as mean ± SEM, $n = 4$ (one-way ANOVA: $p \leqslant 0.0001$); Kruskal–Wallis test: $^{**}p \leqslant 0.0026$ vs control).

3.1.1. 4-Amino-N3-ethyl-2-thioxo-1,3-thiazole-5-carbonitrile (1)

Yield: 74%. White solid; mp: 205 °C. IR (KBr) 3308.95, 3227.11, 2973, 2206.84, 1193.14 cm^{-1}; ^1H NMR ($CDCl_3$): δ ppm 1.27–1.32 (t, J = 7.2 Hz, 3H, CH_3), 4.22–4.29 (q, J = 7.2 Hz, 2H, CH_2), 6.38 (s, 2H, NH_2). LC–MS (m/z): 185 (M^+), 186 (M+1).

3.1.2. 4-Amino-N3-propyl-2-thioxo-1,3-thiazole-5-carbonitrile (2)

Yield: 85%. White solid; mp: 160 °C. IR (KBr): 3319.65, 3234.59, 2205.95, 1198.14 cm^{-1}; ^1H NMR ($CDCl_3$): δ ppm 1.03 (t, J = 7.5, 3H, CH_3), 1.72–1.854 (m, 2H, CH_2), 4.10 (t, J = 7.8 Hz, 2H,CH_2), 4.83 (s, 2H, NH_2); LC–MS (m/z): 199 (M^+), 200 (M+1).

3.1.3. 4-Amino-N3-butyl-2-thioxo-1,3-thiazole-5-carbonitrile (3)

Yield: 84%. Brown solid; mp: 155 °C. IR (KBr): 3320.05, 3234.19, 2208.95, 1199.14 cm^{-1}; ^1H NMR (300 MHz, $CDCl_3$): δ ppm 0.97 (t, J = 7.2 Hz, 3H, CH_3), 1.353–1.476 (m, 2H, CH_2), 1.66–1.74 (m, 2H, CH_2), 4.16 (t, J = 7.8 Hz, 2H, CH_2), 6.120 (s, 2H, NH_2); LC–MS (m/z): 213 (M^+), 214 (M+1).

3.1.4. 4-Amino-N3-(phenylethyl)-2-thioxo-1,3-thiazole-5-carbonitrile (4)

Yield: 75%, yellow solid; mp: 245–246 °C; IR (KBr): 3312, 3188, 2207, 684 cm^{-1}; ^1H NMR (300 MHz, $CDCl_3$): δ ppm 2.94(t, 2H, CH_2), 4.32(t, 2H, CH_2), 6.9(s, 2H, Ar), 7.24–7.33(m, 3H, Ar), 7.79(s, 2H, NH_2); LC–MS (m/z): 263 (M^+), 264 (M+1).

3.1.5. 4-Amino-N3-phenyl-2-thioxo-1,3-thiazole-5-carbonitrile (5)

Yield: 75%. Yellow solid; mp: 286 °C. IR (KBr): 3369, 3230, 2204, 684 cm^{-1}; ^1H NMR (300 MHz, $CDCl_3$): δ ppm 5.90 (s, 2H, NH_2) 7.12–7.47 (m, 5H, Ar); LC–MS (m/z): 233 (M^+).

3.2. General procedure for synthesis of (4*E*)-4-(4-substitutedbenzylideneamino)-N3-substituted-2,3-dihydro-2-thioxothiazole-5-carbonitrile (6–19)

An equimolar mixture of 4-amino-3-substituted-2,3-dihydro-2-thioxothiazole-5-carbonitrile (**1**–**5**) and p-substituted benzaldehyde (3.78 g, 27 mmol) with pinch of $AlCl_3$ was stirred in chloroform for 8 h. After completion of the reaction, the solvent was evaporated. The reaction mixture was dissolved in ethylacetate, washed with water and dried with anhydrous sodium sulfate. Crude product was purified by column chromatography using petroleum ether and ethyl acetate (98:2) as solvent.

3.2.1. (4*E*)-4-(4-Flurobenzylideneamino)-N3-ethyl-2,3-dihydro-2-thioxothiazole-5-carbonitrile (6)

Yield: 65%; yellow solid; mp: 175–177 °C; IR (KBr): 2978, 2934, 2874 (alkyl) 2211 (CN) cm^{-1}; ^1H NMR (400 MHz, $CDCl_3$): δ ppm 1.27 (t, 3H, CH_3), 4.31–4.37 (q, 4H, CH_2), 7.27–7.29 (m, 2H, Ar), 8.02–8.05 (m, 2H, Ar), 8.95 (s, 1H, Ar); ^{13}C NMR ($CDCl_3$): 12.7, 43.0, 112.1, 116.7, 116.9, 130.3, 133.1, 156.6, 165.5, 167.2, 185.9; LC–MS (m/z): 291 (M^+), 292 (M^++1). Analysis calculated for $C_{13}H_{10}FN_3S_2$: C, 53.59; H, 3.46; N, 14.42; S, 22.01; Found: C, 53.48; H, 3.33; N, 14.53; S, 22.17.

3.2.2. (4*E*)-4-(4-Flurobenzylideneamino)-N3-propyl-2,3-dihydro-2-thioxothiazole-5-carbonitrile (7)

Yield: 69%; yellow solid; mp: 135–137 °C; IR (KBr): 2859, 2952 (alkyl) 2206 (CN) cm^{-1}; ^1H NMR (400 MHz, $CDCl_3$): δ ppm 0.92–0.95 (t, 3H, CH_3), 1.74–1.79 (m, 2H, CH_2), 4.18–4.21 (t, 2H, CH_2), 7.21–7.24 (m, 2H, Ar), 7.97–7.99 (m, 2H, Ar), 8.90 (s, 1H, Ar); ^{13}C NMR ($CDCl_3$): 11.2, 20.7, 49.0, 111.9, 116.9, 130.1, 132.8, 132.9, 156.4, 165.8, 166.8, 168.4, 186.1; LC–MS: m/z 306 (M^++1); Analysis calculated for $C_{14}H_{12}FN_3S_2$: C, 55.06; H, 3.96; N, 13.76; S, 21.00; Found: C, 55. 18; H, 3.87; N, 13.86; S, 21.14.

3.2.3. (4*E*)-4-(4-Flurobenzylideneamino)-N3-butyl-2,3-dihydro-2-thioxothiazole-5-carbonitrile (8)

Yield: 75%; yellow solid; mp: 125–127 °C; IR (KBr): 2965, 2932 (alkyl), 2206 (CN) cm^{-1}; ^1H NMR (400 MHz, $CDCl_3$): δ ppm 0.94–0.96 (t, 3H, CH_3), 1.38–1.44 (m, 2H, CH_2), 1.74–1.78 (m, 2H, CH_2), 4.25–4.28 (m, 2H, CH_2), 7.25–7.29 (m, 2H, Ar), 8.01–8.04 (d, 2H, Ar), 8.94 (s, 1H, Ar); ^{13}C NMR ($CDCl_3$): 13.6, 19.9, 29.3, 47.3, 111.9, 116.7, 117.0, 130.1, 132.8, 132.9, 156.4, 165.4, 166.8, 186.0; LC–MS (m/z): 320 (M^++1); Analysis calculated for $C_{15}H_{14}FN_3S_2$: C, 56.40; H, 4.42; N, 13.16; S, 20.08; Found: C, 56.51; H, 4.49; N, 13.27; S, 20.17.

3.2.4. (4*E*)-4-(4-Flurobenzylideneamino)-N3-Phenylethyl-2,3-dihydro-2-thioxothiazole-5-carbonitrile (9)

Yield: 78%; yellow solid. mp: 174–176 °C; IR (KBr): 3078 (aromatic), 2206 (CN) cm^{-1}; ^1H NMR (400 MHz, $CDCl_3$): δ ppm 3.08–3.12 (t, 2H, CH_2), 4.49–4.52 (t, 2H, CH_2), 6.99–7.00 (d, 2H, Ar), 7.14–7.28 (m, 5H, Ar), 7.79–7.82 (m, 2H, Ar) 8.04 (s, 1H, Ar); ^{13}C NMR ($CDCl_3$): 32.4, 48.8, 111.8, 116.5, 116.7, 127.0, 128.7, 129.0, 130.0, 132.6, 132.7, 137.6, 140.6, 156.9, 165.8, 166.6, 185.0. LC–MS (m/z): 367 (M^+), 368 (M^++1); Analysis calculated for $C_{19}H_{14}FN_3S_2$: C, 62.10; H, 3.84; N, 11.44; S, 17.45. Found C, 62.22; H, 3.72; N, 11.32; S, 17.52.

3.2.5. (4*E*)-4-(4-Flurobenzylideneamino)-N3-phenyl-2,3-dihydro-2-thioxothiazole-5-carbonitrile (10)

Yield: 72%; yellow solid; mp: 184–186 °C; IR (KBr): 3075 (aromatic), 2208 (CN) cm^{-1}; ^1H NMR (400 MHz, $CDCl_3$): δ ppm 7.26–7.27 (m, 2H, Ar), 7.51–7.56 (m, 7H, Ar), 8.83 (s, 1H, Ar); ^{13}C NMR ($CDCl_3$): 111.7, 116.5, 116.7, 128.3, 129.5, 130.0, 130.1, 132.7, 132.8, 135.9, 156.9, 165.2, 166.3, 187.4; LC–MS (m/z): 339 (M^+), 340 (M^++1); Analysis calculated for $C_{17}H_{10}FN_3S_2$: C, 60.16; H, 2.97; N, 12.38; S, 18.89. Found C, 60.27; H, 3.07; N, 12.29; S, 18.99.

3.2.6. (4*E*)-4-(4-Chlorobenzylideneamino)-N3-ethyl-2,3-dihydro-2-thioxothiazole-5-carbonitrile (11)

Yield: 68%; yellow solid; mp: 178–180 °C; IR (KBr): 2848, 2922 (alkyl) 2204 (CN) cm^{-1}; ^1H NMR (400 MHz, $CDCl_3$): δ ppm 1.32–1.35 (t, 3H, CH_3), 4.31–4.37 (q, 4H, CH_2), 7.52–7.57 (d, 2H, Ar), 7.94–7.96 (d, 2H, Ar), 8.96 (s, 1H, Ar); ^{13}C NMR ($CDCl_3$): 12.6, 42.9, 111.8, 116.6, 129.4, 129.8, 131.5, 132.1, 141.1, 156.0, 167.2, 185.9; LC–MS (m/z): 308 (M^++1); Analysis calculated for $C_{13}H_{10}ClN_3S_2$: C, 50.72; H, 3.27; N, 13.65; S, 20.83. Found: C, 50.66; H, 3.32; N, 13.72; S, 20.90.

3.2.7. (4*E*)-4-(4-Chlorobenzylideneamino)-3-propyl-2,3-dihydro-2-thioxothiazole-5-carbonitrile (12)

Yield: 72%; yellow solid; mp: 142–144 °C. IR (KBr): 2954, 2974(alkyl), 2211 (CN) cm^{-1}; ^1H NMR (400 MHz, $CDCl_3$) δ ppm 0.91–0.99 (t, 3H, CH_3), 2.07–2.18 (m, 2H, CH_2), 4.21–4.25 (t, 2H, CH_2), 7.25–7.29 (m, 2H, Ar), 8.01–8.03 (m, 2H, Ar), 8.94 (s, 1H, Ar); ^{13}C NMR ($CDCl_3$): 11.2, 20.7, 49.0, 111.9, 116.7, 130.1, 132.8, 132.9, 141.4, 156.4, 166.8, 186.1; LC–MS (m/z): 321 (M^+), 322 (M^++1); Analysis calculated for $C_{14}H_{12}ClN_3S_2$: C, 52.25; H, 3.76; N, 13.06; S, 19.93. Found C, 52.36; H, 3.66; N, 13.12; S, 20.09.

3.2.8. (4*E*)-4-(4-Chlorobenzylideneamino)-N3-butyl-2,3-dihydro-2-thioxothiazole-5-carbonitrile (13)

Yield: 76%; yellow solid; mp: 135–137 °C; IR (KBr): 2856, 2922 (alkyl), 2206 (CN) cm^{-1}; ^1H NMR (400 MHz, $CDCl_3$): δ ppm 0.094–0.095 (t, 3H, CH_3), 1.40–1.43 (m, 2H, CH_2), 1.72–1.78 (m, 2H, CH_2), 4.24–4.28 (t, 2H, CH_2), 7.55–7.579 (d, 2H, Ar), 7.93–7.95 (d, 2H, Ar), 8.95(s, 1H, Ar); ^{13}C NMR ($CDCl_3$): 13.6, 19.9, 29.3, 47.4, 111.8, 116.8, 129.8, 131.5, 132.1, 141.2, 156.2, 166.9, 186.0; LC–MS (m/z): 335 (M^+), 336 (M^++1); Analysis calculated for $C_{15}H_{14}ClN_3S_2$: C, 53.64; H, 4.20; N, 12.51; S, 19.09. Found C, 53.76; H, 4.33; N, 12.40; S, 19.18.

3.2.9. (4*E*)-4-(4-Chlorobenzylideneamino)-N3-phenyl-2,3-dihydro-2-thioxothiazole-5-carbonitrile (14)

Yield: 72%; yellow solid; mp: 187–189 °C; IR (KBr): 3059 (aromatic), 2201 (CN) cm^{-1}; ^1H NMR (400 MHz, $CDCl_3$): δ ppm 7.28–7.30 (m, 2H, Ar), 7.54–7.68 (m, 7H, Ar), 8.86 (s, 1H, Ar); ^{13}C NMR ($CDCl_3$): 111.7, 116.5, 128.3, 128.8, 129.5, 130.0, 130.1, 132.7, 132.8, 135.9, 156.9, 166.3, 187.4; LC–MS (*m*/*z*): 356 (M^++1); Analysis calculated for $C_{17}H_{10}ClN_3S_2$: C, 57.38; H, 2.83; N, 11.81; S, 18.02. Found: C, 57.50; H, 2.72; N, 11.90; S, 18.11.

3.2.10. (4*E*)-4-(4-Bromobenzylideneamino)-N3-ethyl-2,3-dihydro-2-thioxothiazole-5-carbonitrile (15)

Yield: 75%; yellow solid; mp: 182–184 °C; IR (KBr): 2954 (alkyl), 2211 (CN) cm^{-1}; ^1H NMR (400 MHz, $CDCl_3$): δ ppm 1.32–1.35 (t, 3H, CH_3), 4.31–4.36 (q, 4H, CH_2), 7.71 (d, 2H, Ar), 7.86–7.88 (d, 2H, Ar), 8.95 (s, 1H, Ar); ^{13}C NMR ($CDCl_3$): 12.6, 42.9, 111.8, 116.8, 130.0, 131.5, 132.5, 132.8, 156.0, 167.2; 185.8. LC–MS (*m*/*z*): 352 (M^++1); Analysis calculated for $C_{13}H_{10}BrN_3S_2$: C, 44.32; H, 2.86; N, 11.93; S, 18.20. Found: C, 44.41; H, 2.72; N, 12.04; S, 18.32.

3.2.11. (4*E*)-4-(4-Bromobenzylideneamino)-N3-propyl-2,3-dihydro-2-thioxothiazole-5-carbonitrile (16)

Yield: 72%; yellow solid; mp: 155–157 °C; IR (KBr): 2923, 2852 (alkyl), 2210 (CN) cm^{-1}; ^1H NMR (400 MHz, $CDCl_3$): δ ppm 0.90–0.94 (t, 3H, CH_3), 1.72–1.76 (m, 2H, CH_2), 4.16–4.20 (t, 2H, CH_2), 7.67–7.69 (d, 2H, Ar), 7.81–7.82 (d, 2H, Ar), 8.89 (s, 1H, Ar); LC–MS (*m*/*z*): 366 (M^++1); Analysis calculated for $C_{14}H_{12}BrN_3S_2$: C, 45.91, H, 3.30; N, 11.47; S, 17.51. Found: C, 46.02; H, 3.41; N, 11.36; S, 17.59.

3.2.12. (4*E*)-4-(4-Bromobenzylideneamino)-N3-butyl-2,3-dihydro-2-thioxothiazole-5-carbonitrile (17)

Yield: 66%; yellow solid; mp: 138–140 °C; IR (KBr): 2923, 2852 (alkyl), 2211 (CN) cm^{-1}; ^1H NMR (400 MHz, $CDCl_3$): δ ppm 0.94–0.97 (t, 3H, CH_3), 1.36–1.43 (m, 2H, CH_2), 1.73–1.77 (m, 2H, CH_2), 4.24–4.28 (t, 2H, CH_2), 7.72 (d, 2H, Ar), 7.87 (d, 2H, Ar), 8.94 (d, 2H, Ar), 8.94 (s, 1H, Ar); ^{13}C NMR ($CDCl_3$): 13.7, 19.9, 29.2, 47.4, 111.8, 116.7, 129.9, 131.5, 132.6, 132.7, 156.2, 167.2, 185.9; LC–MS (*m*/*z*): 379 (M^+), 380 (M^++1); Analysis calculated for $C_{15}H_{14}BrN_3S_2$: C, 47.37; H, 3.71; N, 11.05; S, 16.86. Found: C, 47.50; H, 3.63; N, 11.14; S, 16.97.

3.2.13. (4*E*)-4-(4-Bromobenzylideneamino)-N3-phenylethyl-2,3-dihydro-2-thioxothiazole-5-carbonitrile (18)

Yield: 79%; yellow solid; mp: 180–182 °C; IR (KBr): 3072 (aromatic), 2202 (CN) cm^{-1}; ^1H NMR (400 MHz, $CDCl_3$): δ ppm 3.08–3.11 (t, 2H, CH_2), 4.48–4.52 (t, 2H, CH_2), 6.97–7.08 (m, 2H, Ar), 7.11–7.28 (m, 3H, Ar), 7.50–7.52 (d, 2H, Ar), 7.71–7.73 (d, 2H, Ar), 8.02 (s, 1H, Ar); ^{13}C NMR (CDCl3): 32.4, 48.8, 111.7, 116.7, 127.0, 128.7, 129.1, 129.5, 131.3, 132.1, 137.6, 140.8, 156.7, 165.9, 185.9; LC–MS (*m*/*z*): 429 (M^++1); Analysis calculated for $C_{19}H_{14}BrN_3S_2$: C, 53.27; H, 3.29; N, 9.81; S, 14.97. Found: C, 53.39; H, 3.38; N, 9.92; S, 14.86.

3.2.14. (4*E*)-4-(4-Bromobenzylideneamino)-N3-phenyl-2,3-dihydro-2-thioxothiazole-5-carbonitrile (19)

Yield: 72%; yellow solid; mp: 185–187 °C; IR (KBr): 3065 (aromatic), 2208 (CN) cm^{-1}; ^1H NMR (400 MHz, $CDCl_3$): δ ppm 7.27–7.28 (m, 2H, Ar), 7.51–7.60 (m, 7H, Ar), 8.85 (s, 1H, Ar); ^{13}C NMR ($CDCl_3$): 117.7, 116.8, 128.3, 129.5, 129.5, 129.8, 130.0, 131.4, 132.5, 132.6, 135.8, 156.7, 166.6, 187.3; LC–MS (*m*/*z*): 400 (M^++1); Analysis calculated for $C_{17}H_{10}BrN_3S_2$: C, 51.01; H, 2.52; N, 10.50; S, 16.02. Found C, 51.19; H, 2.60; N, 10.38; S, 16.14.

3.3. Molecular docking

Docking simulations were performed with AutoDock3.0.5 according to our previous report.[18] The recently solved X-ray crystal structure of the human A2AR (pdb code: 3EML; 2.6 Å resolution) in complex with ZM241385 was retrieved from the RCSB Protein Data Bank and all heteroat-oms were removed. The $A_{2A}R$ was set up for docking with standard protocol. Polar hydrogens were added using PROTONATE utility distributed with AutoDock3.0.5 then protein co-ordinates were subjected to minimize with CHARMm force field potential.[21,22] Steps (1000) of steepest descent followed by conjugate gradient minimization until the RMS gradient of the potential energy was less than 0.05 kJ mol^{-1} $Å^{-1}$ performed the minimizations. Kollman united atom charges and solvation parameters were added to the final protein file. The known $A_{2A}R$ antagonists and thiazole derivatives were drawn on BUILDER module (insight II). DISCOVER molecular dynamics (CHARMm force field) was run to carry the optimization of the ligands, which were saved in mol2 format with the aid of BABEL programs (Pat Walters and Matt Stahl, NCI). Full hydrogens were added to the ligands and Gasteiger–Marsili partial atomic charges were computed using the BABEL program and saved in the PDBQ format. All possible flexible torsions of the resultant ligand molecules were defined by using AUTOTORS. The prepared ligands in PDBQ format were used as input files for AutoDock3.0.5 in the next step. Docking simulation was carried out using the Lamarckian Genetic Algorithm.[21] For binding energy, three terms were taken into account in the docking step: the van der Waals interaction represented as a Lennard–Jones 12–6 dispersion/repulsion term, the hydrogen bonding represented as a directional 12–10 term, and the Coulombic electro-static potential. The resulting docking orientations lying within 2.0 Å in the root-mean square deviation (rmsd) tolerance of each other were clustered together represented by the result with the most favorable free energy of binding. Finally, the obtained top-posed docking conformations were subjected to post-docking energy minimization on insight-II/accelrys.[22]

3.4. Radioligand binding assay

Adenosine $A_{2A}R$ and A_1R binding assays: [^{3}H]ZM241385 and [^{3}H]DPCPX binding assays for adenosine $A_{2A}R$ and A_1Rs, respectively, were performed in transfected HEK293T cells with human $A_{2A}R$ and A_1R according Luthra et al.[16] Briefly, 10 μg HEK293T cell membranes isolated from were incubated with different concentrations (1 pM–1 μM) of compounds and 1 nM [^{3}H]ZM241385 in 200 μl incubation buffer containing 50 mM Tris–Cl, 1 mM EDTA, pH 7.4 and 2.5 U/ml adenosine deaminase. Adenosine A_1R assay were performed on 10 μg of HEK293T cell membranes expressing human adenosine A_1Rs and 1 nM [^{3}H]DPCPX in 200 μl incubation buffer. Reactions were carried out for 60 min at 26 °C and were terminated by rapid filtration over 96-well plates equipped with GF/B filters (Milipore, USA). Filters were washed three times with 300 μl of cold washing buffer containing 50 mM Tris–Cl, 10 mM $MgCl_2$, pH 7.4, air dried, and radioactivity retained on filters were counted in 1450 LSC & Luminescence counter (Wallac Microbeta Trilux, Perkin–Elmer, USA). The K_d values for radioligands [^{3}H]ZM241385 and [^{3}H]DPCPX were 0.99 and 1.79 nM, respectively, obtained by saturation binding assays. Nonspecific binding for adenosine $A_{2A}R$ and A_1R was determined in the presence of 50 μM NECA and 50 μM CPA, respectively. Assays were performed in duplicates and compounds were tested thrice. Data were fitted in one site competition-binding model for IC_{50} determination using the program GraphPad Prism 4.0 (GraphPad Software, Inc., San Diego, CA). K_i Values were calculated using Cheng and Prusoff formula.[23]

3.5. Functional assay

HEK293T cells (1×10^6/ml) washed with ice-cold PBS (pH 7.4) were treated with adenosine deaminase (2 U/ml) for 30 min at room temperature (to remove endogenously present adenosine in the cells), followed by treatment with 1 μM standard $A_{2A}R$ agonist (NECA) separately in three eppendorf tubes. The tubes were incubated for 15 min in CO_2 incubator to stimulate the cAMP release, 1 μM of each PTTP and SCH58261 was added to the two tubes and incubated for 15 min. The concentration of the cAMP in the samples was determined according to Luthra et al.[18]

4. Animals

Adult Swiss Albino male mice (4–6 weeks, 20–30 g) were procured from National Institute of Communicable Diseases, Delhi, India and were kept under controlled conditions of temperature (22 ± 1 °C), humidity (60 ± 5%), and illumination (12 h light; 12 h darkness) at the animal house, Dr. B.R. Ambedkar Centre for Bio-medical Research, University of Delhi, Delhi, India. The experimental protocol met the National Guidelines on the 'Proper Care and Use of Animals in Laboratory Research' (Indian National Science Academy, New Delhi) and was approved by the Animal Ethics Committee of the department. The procedures adhered to the NIH Guidelines for the Care and Use of Laboratory Animals.

4.1. Drugs

Haloperidol and SCH58261 were purchased from Sigma Chemicals Co. (St. Louis, Mo) and Tocris Bioscience, respectively. Double distilled filtered and deionized water (Milli-Q-system Waters, Milford, MA) was used throughout the study. Haloperidol, SCH58261 and compounds **6**–**19** were dissolved in 1% acacia in saline. Mice were divided into seven groups of four mice each. SCH58261 (10 mg/kg) and compound **19** (5, 10 and 20 mg/kg) were administered ip to each mice of the assigned group. Saline and 1% acacia in saline were injected to two control groups. After 30 min of pre-treatment, haloperidol (2.5 mg/kg) was injected to one group and all pre-treated groups.

4.2. Catalepsy

The inability of an animal to correct an externally imposed posture (catalepsy score) was measured at different time intervals with both limbs on a square wooden block (3 cm high) by placing the animals on a flat horizontal surface.[18] The length of time that animals held the bar without any voluntary movement was recorded, with a cutoff time of 3 min. Catalepsy score of each mice in a group was taken to compute the mean value of the group.

4.3. Statistical analysis

The data for behavioral studies were statistically evaluated for significance employing nonparametric analysis of variance (Kruskal–Wallis test) for catalepsy and akinesia employing statistical package, Graph Pad Prism 4.0. Values of $p \leqslant 0.05$ were considered significant. Results are given as mean ± SEM values.

Acknowledgments

P.M.L. is thankful to Council of Scientific and Industrial Research (CSIR), Delhi, India, for Grant-in-aid to carry this work. The students C.B.M., A.P., N.K. and N.K. are thankful to CSIR, Delhi, India, for providing the financial support.

Supplementary data

Supplementary data associated with this article can be found, in the online version, at http://dx.doi.org/10.1016/j.bmc.2013.07.005.

References and notes

1. Snyder, S. H. *Neuroscience* **1985**, *8*, 103.
2. Fredholm, B. B.; IJzerman, A. P.; Jacobson, K. A.; Klotz, K. N.; Linden, J. *Pharmacol. Rev.* **2001**, *53*, 527.
3. Chen, J. F.; Fredduzzi, S.; Bastia, E.; Yu, L.-Q. *Neurology* **2003**, *61*, 74.
4. Jenner, P. *Neurology* **2003**, *61*, S38.
5. Mori, A.; Shindou, T.; Ichimura, M.; Nonaka, H.; Kase, H. *J. Neurosci.* **1996**, *16*, 605.
6. Hauser, R. A.; Hubble, J. P.; Truong, D. D. *Neurology* **2003**, *61*, 297.
7. Baraldi, P. G.; Cacciari, B.; Spalluto, G.; Pineda de Villatoro, M. J.; Zocchi, C.; Dionisotti, S.; Ongini, E. *J. Med. Chem.* **1996**, *39*, 1164.
8. Baraldi, P. G.; Cacciari, B.; Romagnoli, R.; Spalluto, G.; Monopoli, A.; Ongini, E.; Varani, K.; Borea, P. A. *J. Med. Chem.* **2002**, *45*, 115.
9. http://www.kyowa-kirin.co.jp/english/news/2009/e2009011501.html.
10. Kisselgof, E.; Tulshian, D. B.; Arik, L.; Zhang, H.; Fawzi, A. *Bioorg. Med. Chem. Lett.* **2005**, *15*, 2119.
11. Jeremiah, J. H.; Roubert, V.; Dolo, C.; Charnet, C.; Spinnewyn, B.; Cornet, S.; Rolland, A.; Marin, J. G.; Bigg, D.; Chabrier, P. E. *Bioorg. Med. Chem. Lett.* **2004**, *14*, 157.
12. Lockhart, B.; Roger, A.; Bonhomie, N.; Goldstein, S.; Lestage, P. *Eur. J. Pharmacol.* **2005**, *511*, 127.
13. Dinakaran, V. S.; Bomma, B.; Der Srinivasan, K. K. *Der Pharm. Chem.* **2012**, *4*, 265.
14. Storch, A.; Burkhardt, K.; Ludolph, A. C.; Schwarz, J. *J. Neurochem.* **2000**, *75*, 2259.
15. Alanine, A.; Flohr, A.; Miller, A. K.; Norcross, R. D.; Riemer, K. U.S. Patent US20,060,003,986A1, 2006.
16. Luthra, P. M.; Mishra, C. B.; Jha, P. K.; Barodia, S. K. *Bioorg. Med. Chem. Lett.* **2010**, *3*, 1214.
17. Luthra, P. M.; Mishra, C. B. U.S. Patent Appl. US2012/264937, 2012.
18. Mishra, C. B.; Barodia, S. K.; Prakash, A.; Kumar, J. B. S.; Luthra, P. M. *Bioorg. Med. Chem.* **2010**, *18*, 2491.
19. Barodia, S. K.; Mishra, C. B.; Prakash, A.; Kumar, J. B. S.; Kumari, N.; Luthra, P. M. *Neurosci. Lett.* **2011**, *488*, 1.
20. Luthe, G.; Jacobus, J. A.; Robertson, L. W. *Environ. Toxicol. Pharmacol.* **2008**, *25*, 202.
21. Morris, G. M.; Goodsell, D. S.; Halliday, R. S.; Huey, R.; Hart, W. E.; Belew, K. R.; Olson, A. J. *J. Comput. Chem.* **1998**, *19*, 1639.
22. Accelrys Inc., Forcefield-based Simulations, Accelrys Inc., San Diego, 2002, URL http://www.accelrys.com/doc/life/insight2000.1/ffbs/FFSimulTOC.html.
23. Cheng, Y.; Prusoff, W. H. *Biochem. Pharmacol.* **1973**, *22*, 3099.